

# Aluminum Deoxidation Equilibria in Liquid Iron: Part I. Experimental



MIN-KYU PAEK, JUNG-MOCK JANG, YOUN-BAE KANG, and JONG-JIN PAK

In order to provide accurate information for refining of steel containing more than 1 mass pct Al, previously known information about Al deoxidation equilibria in liquid iron was critically reviewed. New Al deoxidation equilibria, Al and O contents in liquid iron in equilibrium with solid  $\text{Al}_2\text{O}_3$  were measured at 1873 K and 1923 K (1600 °C and 1650 °C) over the whole Al composition range,  $0.0027 < [\text{pct Al}] < 100$ . In order to secure the deoxidation equilibria, in the present study, the Al deoxidation experiments were carried out by employing three different methods: (1) traditional Al deoxidation by the addition of Al into Fe-O alloys, (2) oxidation of Al in Fe-Al alloys by the addition of  $\text{Fe}_2\text{O}_3$  as an oxygen source, and (3) addition of CaO flux for an effective removal of suspended  $\text{Al}_2\text{O}_3$  inclusions in liquid alloys containing high Al. In addition, in the present study, the O solubility limit in pure Al melt in equilibrium with solid  $\text{Al}_2\text{O}_3$  was also measured in the temperature range from 1673 K to 1873 K (1400 °C to 1600 °C). The present experimental results provide a complete set of Al deoxidation equilibria in liquid iron which may be useful for the estimation of residual oxygen level and alumina inclusion formation in high Al steel processing. Interaction parameter formalism, which was originally proposed by Wagner and Chipman and has been widely used to interpret the Al deoxidation equilibria in liquid iron, was found to be inapplicable. Limitation of the interaction parameter formalism at high Al content in liquid Fe was discussed.

DOI: 10.1007/s11663-015-0368-0

© The Minerals, Metals & Materials Society and ASM International 2015

## I. INTRODUCTION

ALUMINUM deoxidation equilibria in liquid iron containing Al up to hundreds of ppm have been well investigated for typical Al-killed steels by the various experimental techniques<sup>[1–11]</sup> and theoretical studies.<sup>[12–16]</sup> Recently, the deoxidation limit of some high Al-alloyed steels has also received great attention, because new Advanced High Strength Steels (AHSS) containing Al up to 3 mass pct such as Transformation-Induced Plasticity (TRIP) or Twinning-Induced Plasticity (TWIP) steels have been developed for future automotive industry. They provide an excellent combination of high strength, high ductility, and high formability over conventional steels.<sup>[17,18]</sup> For the production of such steel grades, thermodynamic information on the Al deoxidation equilibria in liquid iron is urgently needed. However, the experimental results of Al-O relation in liquid iron in high Al concentration region have been found inconsistent. The oxygen content in high Al-containing steel has not been well established.<sup>[11]</sup>

MIN-KYU PAEK, formerly Graduate Student, with Department of Materials Engineering, Hanyang University, ERICA, Ansan 426-791, Republic of Korea, is now a post-doctor, with the Department of Mining and Materials Engineering, McGill University, Montreal, QC, H3A 2B2, Canada. JUNG-MOCK JANG, Graduate Student, and JONG-JIN PAK, Professor, are with the Department of Materials Engineering, Hanyang University Contact e-mail: jipak@hanyang.ac.kr YOUN-BAE KANG, Associate Professor, is with the Graduate Institute of Ferrous Technology, Pohang University of Science and Technology, Pohang, Kyungbuk, 790-784, Republic of Korea.

Manuscript submitted November 19, 2014.

Article published online May 20, 2015.

Phases of inclusions in high Mn-high Al steel still need clarification due to accurate deoxidation equilibria.<sup>[19]</sup>

As known, the analytical solution of the deoxidation equilibria, in particular for those of Al in steel, has been described by the interaction parameter formalism,<sup>[20]</sup> originally proposed by Wagner<sup>[21]</sup> based on theory proposed by Chipman.<sup>[22]</sup> Due to its simple concept and equation, it has enjoyed much popularity, and this has shown acceptable results at low Al content in the steel, particularly lower than 0.1 mass pct. However, as the Al concentration increases, the Wagner's Interaction Parameter Formalism (WIPF) does not show satisfactory result.<sup>[4–6,9,10]</sup> For the practical application at high Al content, it is now necessary to consider an improved way to account for the Al deoxidation equilibria.

The present study is an attempt to measure accurate deoxidation equilibria of Al in liquid iron from almost no Al to pure Al for the first time. In the present study, three different types of experimental techniques were employed depending on the Al content in liquid iron; Al deoxidation by the addition of Al (0.0027 to 17.3 mass pct Al), oxidation of Al by the addition of  $\text{Fe}_2\text{O}_3$  (8.04 to 0.0454 mass pct Al), and the addition of CaO flux (>20 mass pct Al). Details of experimental techniques will be explained in Section III. All the experimental data regarding Al deoxidation in Fe-Al-O system are reported in the present article (Part I). In order to analytically interpret the Al deoxidation equilibria obtained in the present study as well as those available and reliable in literature,<sup>[1–11]</sup> a new thermodynamic modeling was carried out by the present authors for the Fe-Al-O alloy

taking into account the strong chemical interaction between Fe/Al and O in the framework of CALculation of PHase Diagram (CALPHAD). This will be presented in the second part of the present series (Part II).<sup>[23]</sup> In the third part of the present series (Part III),<sup>[24]</sup> the experimental work and thermodynamic modeling were extended to contain Mn in the Fe-Al-O alloys.

## II. LITERATURE SURVEY

Information regarding Al deoxidation in liquid steel from literature is categorized into “experimental measurement” and “thermodynamic analysis.” In most cases, researchers reporting the experimental data also provided their own thermodynamic analysis, mostly based on WIPF. The Al deoxidation equilibria, represented by equilibrium concentration of Al and O in liquid iron in equilibrium with solid  $\alpha$ -Al<sub>2</sub>O<sub>3</sub> (hereafter, Al<sub>2</sub>O<sub>3</sub>), have been experimentally measured several times over decades. Those experimental data are shown in Figure 1, along with calculated deoxidation curves by several authors.<sup>[5,10,11,13,16]</sup> The deoxidation equilibria have been measured by various experimental and analytical methods under different temperatures and compositions, and are summarized in Table I. As can be seen in the figure, there have been huge discrepancies among the experimental results and calculations.

### A. Experimental Measurement

Deoxidation equilibria were measured mostly by equilibrating liquid Fe-Al alloy with solid Al<sub>2</sub>O<sub>3</sub> and/or gas phase. Equilibrium concentrations of Al and O were measured, and some researchers also measured equilibrium oxygen partial pressure exerted on the liquid alloys.<sup>[1,2]</sup> Oxygen potential in liquid alloys was sometimes measured employing electrochemical technique.<sup>[4,6,9]</sup> Composition of O was generally analyzed either by vacuum fusion method, neutron activation method, or inert gas fusion method, while that of Al was obtained by wet-chemical analysis. Experimental diffi-

culty mostly lies on accurate determination of chemically dissolved O content without overestimation due to insoluble O from suspended oxide particles. Supersaturation of O in the liquid alloy was also discussed to be a source of error.<sup>[8]</sup> The other concern is that, during the analysis of O in the sample containing high Al, the O content might be underestimated by formation of AlO(g) or Al<sub>2</sub>O(g) gas species, while the sample is subjected to melt under inert gas or vacuum (gettering effect).<sup>[25]</sup> Another problem to be mentioned is “oxygen deficiency” in the high Al-containing melt due to a lack of available oxygen when a large amount of Al is added to the melt as pointed out by Yin.<sup>[26]</sup> When the Al is continuously added into the melt, O in the melt would be consumed continuously and reach a minimum as shown in the deoxidation curve. This would lead a lack of O source to take part in the deoxidation equilibrium at higher Al contents. In such situation, the equilibrium O content at high Al content would be underestimated.<sup>[26]</sup> All these difficulties have resulted in a wide scatter of the Al deoxidation equilibria as shown in Figure 1.

In order to eliminate the experimental difficulties and the analytical errors, Rohde *et al.*<sup>[5]</sup> tried to measure Al deoxidation equilibria by adding CaO-Al<sub>2</sub>O<sub>3</sub> flux on top of liquid iron at 1873 K (1600 °C). They also measured the deoxidation equilibria without the flux. They confirmed that the use of flux on top of the liquid iron, being melted, significantly decreased analytical uncertainty. They explained that the O content was close to the theoretical equilibrium value by the addition of flux, and this was because the alumina particles generated in the liquid iron could be removed to the metal/molten flux interface, thereby reducing possibility of overestimation of the O content by the alumina particles in the melt. They explained that the flux was saturated with Al<sub>2</sub>O<sub>3</sub> after the equilibrium reaction and assumed that the activity of Al<sub>2</sub>O<sub>3</sub> was unity.<sup>[5]</sup> The Japan Society for the Promotion of Science (JSPS)<sup>[27]</sup> recommended the Rohde *et al.*<sup>[5]</sup>’s results. Suito *et al.*<sup>[8]</sup> also carried out Al deoxidation experiments with or without flux. However, no distinct difference was found among their experimental results of the Al-O relation.

Fruehan,<sup>[4]</sup> Janke and Fischer,<sup>[6]</sup> and Dimitrov *et al.*<sup>[9]</sup> have directly determined the O activity by the Electro Motive Force (EMF) technique, while O content was separately determined. At low Al concentration, the O content decreased with increasing Al content and agreed well with the O activity data directly determined by EMF measurements. Further increase of the Al content increased the O content, showing a minimum on the deoxidation curve.

At high Al content over 1 mass pct, a few of investigations were reported, showing a huge scatter as shown in Figure 1. Inoue *et al.*<sup>[25]</sup> analyzed the O content in the Fe-Al alloy samples according to the flux type, analytical temperature, and heating pattern of the apparatus, and suggested the best way for the oxygen analysis at high Al concentration from 10 to 15 mass pct. Kang *et al.*<sup>[11]</sup> also tested the various conditions of the O analysis in Fe-5-9 mass pct Al alloys, such as Ni capsule, Ni bath, and temperature, but there was no significant difference in the O content for

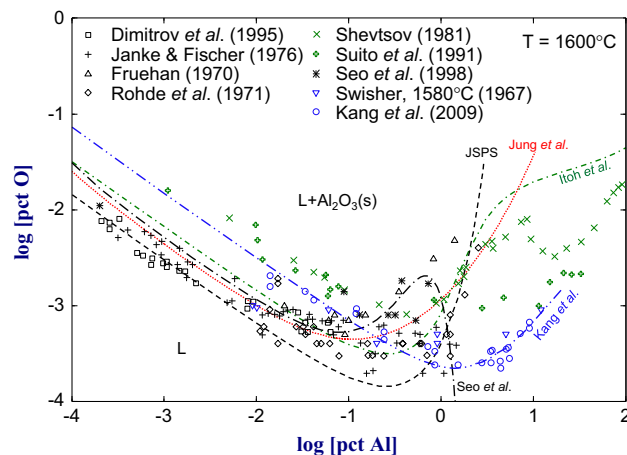


Fig. 1—The Al-O relations in liquid iron at 1873 K (1600 °C): Symbols are experimental data<sup>[3–11]</sup> and lines are thermodynamic calculations.<sup>[5,10,11,13,16]</sup>

**Table I. Investigations for the Al Deoxidation Equilibria in Liquid Iron**

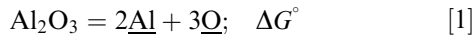
Author	Year	Experimental Method/[pct O] Analysis	Temp. [K (°C)] [pct Al] Range	log $K$ [1873 K (1600°C)] $e_{\text{O}}^{\text{Al}}$ [1873 K (1600°C)]	Ref.
Gokcen and Chipman	1953	H <sub>2</sub> -H <sub>2</sub> O/V	1968 K to 2139 K (1695 °C to 1866 °C)	-13.69	1
McLean and Bell	1965	H <sub>2</sub> -H <sub>2</sub> O/V	0.003 to 0.057 1996 K to 2096 K (1723 °C to 1823 °C)	-12 -13.9	2
Swisher	1967	Fe(l)-Al <sub>2</sub> O <sub>3</sub> (s)/V	0.003 to 0.067 1853 K (1580 °C)	-4.6 —	3
Fruehan	1970	EMF/N	0.009 to 12 1873 K (1600 °C)	— -13.35	4
Rohde	1971	Fe(l)-CaO-Al <sub>2</sub> O <sub>3</sub> slag	0.02 to 1.4 1873 K to 2023 K (1600 °C to 1750 °C)	-3.9 -13.57	5
Janke and Fischer	1976	EMF	0.01 to 2.5 1873 K (1600 °C)	-1.17 -13.62	6
Shevtsov	1981	Fe(l)-Al <sub>2</sub> O <sub>3</sub> (s)/V	0.0003 to 1.3 1873 K (1600 °C)	-1.0 —	7
Suito <i>et al.</i>	1991	Fe(l)-Al <sub>2</sub> O <sub>3</sub> (s), Fe(l)-CaO-Al <sub>2</sub> O <sub>3</sub> slag/I	0.01 to 100 1873 K (1600 °C)	— —	8
Dimitrov <i>et al.</i>	1995	EMF	0.001 to 32.7 1873 K (1600 °C)	— -14.01	9
Seo <i>et al.</i>	1998	Fe(l)-Al <sub>2</sub> O <sub>3</sub> (s)/I	0.0001 to 1.2 1873 K (1600 °C)	-5.54 -12.96	10
Kang <i>et al.</i>	2009	Fe(l)-Al <sub>2</sub> O <sub>3</sub> (s)/I	0.0002 to 1.0 1873 K (1600 °C)	-4.09 -11.52	11
Paek <i>et al.</i>	2015	Fe(l)-Al <sub>2</sub> O <sub>3</sub> (s), Fe(l)-CaO-Al <sub>2</sub> O <sub>3</sub> slag/I	0.01 to 10 1873 K to 1923 K (1600 °C to 1650 °C)	-0.23 —	present study
			0.0027 to 100	—	

V, vacuum fusion method; N, neutron activation; I, inert gas fusion-infrared absorptiometry.

the analysis using the inert gas fusion-infrared absorptiometry. Above 10 mass pct Al in liquid iron, results of Shevtsov<sup>[7]</sup> and Suito *et al.*<sup>[8]</sup> are available. As shown in Figure 1, Shevtsov<sup>[7]</sup> reported two minima on the deoxidation curve. He suggested that one minimum at the high Al content was due to the formation of alumina spinel, “Al<sub>3</sub>O<sub>4</sub>” instead of Al<sub>2</sub>O<sub>3</sub>, which was likely to be metastable phase.

### B. Thermodynamic Analysis

Reaction for the deoxidation by Al in liquid iron is written as



The equilibrium constant of the Reaction [1] can be expressed as

$$\begin{aligned} \log K &= -\Delta G^\circ / 2.303RT = \log h_{\text{Al}}^2 \cdot h_{\text{O}}^3 \\ &= 2 \log f_{\text{Al}} + 3 \log f_{\text{O}} + 2 \log [\text{pctAl}] + 3 \log [\text{pctO}] \end{aligned} \quad [2]$$

where  $h_i$  and  $f_i$  are the activity and activity coefficient of  $i$  in liquid iron with respect to 1 mass pct standard state, respectively. Activity of Al<sub>2</sub>O<sub>3</sub> was set to unity. Traditionally, WIPF has been actively used to estimate the  $f_i$  along with first-order interaction parameters, and Eq. [2] can be rewritten as

$$\begin{aligned} \log K &= 2(e_{\text{Al}}^{\text{Al}}[\text{pctAl}] + e_{\text{Al}}^{\text{O}}[\text{pctO}]) \\ &+ 3(e_{\text{O}}^{\text{Al}}[\text{pctAl}] + e_{\text{O}}^{\text{O}}[\text{pctO}]) \\ &+ 2 \log [\text{pctAl}] + 3 \log [\text{pctO}] \end{aligned} \quad [3]$$

where  $e_i^j$  is the first-order interaction parameter of  $j$  on  $i$  in liquid iron in mass pct. Using the Lupis’ reciprocal relationship,<sup>[20]</sup> Rohde *et al.*<sup>[5]</sup> determined the  $e_{\text{O}}^{\text{Al}}$  as -1.17, -0.83, and -0.72 at 1873 K, 1923 K, and 1973 K (1600 °C, 1650 °C, and 1700 °C), respectively, along with the  $\log K = -64,000/T + 20.57$ . As shown in Figure 1, the Al deoxidation curve calculated using the parameter of Rohde *et al.*<sup>[5]</sup> adopted by JSPS shows a good agreement with the experimental data up to a few hundreds ppm of Al. This was practically acceptable as most typical low C-Al-killed steels contain Al up to a maximum of 600 ppm. The calculations adopted by JSPS show a minimum at higher Al concentration on the deoxidation curve, and then show a rapid increase of the [pct O].

Later, Itoh *et al.*<sup>[13]</sup> employed the second-order interaction parameters to extend the applicability of the WIPF toward higher Al content. They also revised the  $K$  value which is suitable to explain the experimental data with their estimated first-/second-order interaction parameters. Using the Lupis’ reciprocal relationship,<sup>[20]</sup> the relations between the first- and second-order interaction parameters can be derived as

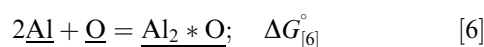
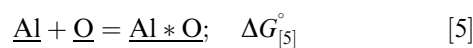
$$\begin{aligned}
& \{ \log K - (2[\text{pct Al}] + 0.02[\text{pct Al}][\text{pct O}])e_{\text{Al}}^{\text{Al}} \\
& - (3[\text{pct Al}] + 3.38[\text{pct O}] - 0.0638[\text{pct Al}][\text{pct O}])e_{\text{O}}^{\text{Al}} \\
& - (3[\text{pct O}] + 0.03[\text{pct Al}][\text{pct O}])e_{\text{O}}^{\text{O}} - \log[\text{pct Al}]^2[\text{pct O}]^3 \} / \\
& (6.74[\text{pct Al}][\text{pct O}] + 3[\text{pct Al}]^2) \\
& = r_{\text{O}}^{\text{Al}} + \frac{(3.57[\text{pct Al}][\text{pct O}] + 2[\text{pct O}]^2)}{(6.74[\text{pct Al}][\text{pct O}] + 3[\text{pct Al}]^2)} r_{\text{Al}}^{\text{O}} \quad [4]
\end{aligned}$$

Itoh *et al.*<sup>[13]</sup> determined the second-order interaction parameters,  $r_{\text{Al}}^{\text{Al}}$  and  $r_{\text{Al}}^{\text{O}}$ , from the  $y$ -intercept and slope of Eq. [4] (when it is plotted as the left-hand side vs the second term in the right hand side except for  $r_{\text{Al}}^{\text{O}}$ ), respectively, using the first-order interaction parameters reported by Rohde *et al.*<sup>[5]</sup> The calculated curves by Itoh *et al.*<sup>[13]</sup> show generally as good as that without the second-order interaction parameter (JSPS), and the calculated O content at high Al concentration increases less significantly compared to that of JSPS. However, at high [pct Al] about 2 to 3 mass pct, the calculated curve shows a very distinct inflection. This is considered to be a mathematical artifact due to the introduction of the second-order interaction parameters.<sup>[15]</sup> A similar calculation by Seo *et al.*<sup>[10]</sup> employing the other set of first-/second-order interaction parameters even exhibited a maximum [pct O] apart from a minimum [pct O] on the deoxidation curve. As the deoxidation curve shown in the figure is indeed a liquidus of  $\text{Al}_2\text{O}_3$  single phase at a given temperature, it is generally unlikely to have a minimum and a maximum simultaneously on a liquidus. These results imply that the use of WIPF cannot be extended toward high Al concentration region with high confidence.

A recent application of the WIPF by Kang *et al.*<sup>[11]</sup> to the deoxidation equilibria at high Al content shows a good agreement with their own measurement up to ~10 mass pct of Al, but did not agree with the most experimental data at low Al content.

Such disagreement between the experimental data and the calculations using the WIPF stems from the fact that (1) the WIPF is, in principle, only applicable to infinite dilute solutions,<sup>[28]</sup> (2) the WIPF considers Al and O as components, and inherently assumes a random mixing between Al and O in liquid iron although there is extremely strong attraction.

In order to overcome these limitations, Bouchard and Bale<sup>[15]</sup> attempted a new approach. They employed the Unified Interact Parameter Formalism (UIPF) proposed by Pelton and Bale,<sup>[29]</sup> which is a modification of WIPF to make it thermodynamically consistent even at higher concentration. Also to take into account the strong interaction between Al and O, the following reactions were considered:



by setting  $\Delta G_{[5]}^{\circ}$  and  $\Delta G_{[6]}^{\circ}$  being negative enough to allow the formation of associates. In the UIPF, the associates  $\text{Al} * \text{O}$  and  $\text{Al}_2 * \text{O}$  and unassociated (or free) Al and O were treated to mix randomly. This is equivalent to use the associate solution model<sup>[15]</sup> with Fe, Al, O, AlO, and  $\text{Al}_2\text{O}$  as model components in Fe-rich corner. In their model calculation, they were able to represent the deoxidation equilibria successfully by eliminating the previous mathematical artifact, *i.e.*, maximum on the deoxidation curve. This concept has been extensively applied by Jung *et al.*<sup>[16]</sup> for multicomponent liquid steel. They applied this model not only for deoxidation by Al but also for various deoxidizing elements such as B, Ba, Ca, Cr, Mg, Mn, Si, Ti, V, *etc.*, and obtained remarkable agreement between the model calculation and available experimental data. However, validity of their calculations for Al deoxidation (as well as deoxidation by other elements) does not extend to Al concentration higher than 5 mass pct, because inherent limit of the model used (interaction parameter formalism).

In conclusion, the literature indicates that equilibrium data of the Al deoxidation at higher Al concentrations still need to be clarified, and a more advanced thermodynamic model is necessary to describe the Al deoxidation equilibria in liquid iron over a wide composition range.

### III. EXPERIMENTAL

The Al deoxidation equilibria were determined at 1873 K and 1923 K (1600 °C and 1650 °C) by measuring the O and Al content in liquid iron in equilibrium with pure solid  $\text{Al}_2\text{O}_3$ . 500 grams of high-purity electrolytic iron (99.99 pct purity, 60 mass ppm O, <5 mass ppm N, 18 mass ppm C, <5 mass ppm Si, <7 mass ppm Ni, 1 mass ppm Al) contained in an  $\text{Al}_2\text{O}_3$  crucible (OD 56 mm, ID 50 mm, H 96 mm) were melted by a 15 kW/30 kHz high-frequency induction furnace. After melting the iron, the melt temperature was directly measured by a Pt/Pt-13 mass pct Rh thermocouple sheathed with an alumina tube (OD 8 mm) immersed in the melt, and the temperature was accurately controlled within 2 °C by a proportional-integral-derivative (PID) controller. After the melt temperature was reached at a desired value, Ar-10 pct  $\text{H}_2$  gas was blown onto the melt surface at a high flow rate of ~2 L/min for 2 hours. The O content in the melt decreased to a value in the range of 8 to 13 mass ppm at 1873 K (1600 °C), and 19 to 24 mass ppm at 1923 K (1650 °C). Then, the gas was switched to dehydrated and deoxidized Ar gas. The flow rate of the gas was adjusted to 0.5 L/min.

In the present study, the Al-O relation was determined over the whole Al composition range,  $0.0027 < [\text{pct Al}] < 100$  in liquid iron. Depending on the Al content in liquid iron, different experimental techniques were employed as summarized in Table II. For the Al range of  $0.0027 < [\text{pct Al}] < 20$ , the Al-O relation in liquid iron was determined by the addition of Al in Fe-O melt as well as the oxidation of Al from its

**Table II. Equilibrium Al and O Contents in Liquid Iron at 1873 K and 1923 K (1600 °C and 1650 °C) Measured by Different Methods**

Temp.[K (°C)]	Exp. No	Method	[pct Al]	[pct O]
1873 (1600)	A-0	Al addition	0	0.00105
	A-1		0.00320	0.00187
	A-2		0.0111	0.00093
	A-3		0.0201	0.00080
	A-4		0.0330	0.00047
	A-5		0.130	0.00028
	A-6		0.217	0.00025
	A-7		0.710	0.00019
	A-8		1.99	0.00023
	A-9		3.06	0.00025
	A-10		5.76	0.00039
	A-11		8.88	0.00094
	A-12	17.3	0.00200	
	B-0	Fe <sub>2</sub> O <sub>3</sub> addition	9.06	0.00018
	B-1		8.04	0.00098
	B-2		7.72	0.00089
	B-3		6.64	0.00092
	B-4		4.48	0.00049
	B-5		2.69	0.00029
	B-6		1.64	0.00028
B-7	0.109		0.00036	
B-8	0.0454	0.00046		
C-1	CaO addition	33.2	0.00473	
C-2		36.6	0.00442	
C-3		49.0	0.00846	
C-4		100	0.0133	
1923 (1650)	D-0	Al addition	0	0.00213
	D-1		0.00266	0.00327
	D-2		0.00864	0.00141
	D-3		0.0296	0.00102
	D-4		0.0870	0.00059
	D-5		0.424	0.00027
	D-6		0.835	0.00021
	D-7		1.71	0.00039
	D-8		2.57	0.00030
	D-9		3.46	0.00043
	D-10		4.64	0.00055
	D-11		6.88	0.00103
	D-12		9.20	0.00149
	D-13	17.2	0.00251	
E-1	CaO addition	45.0	0.00697	

high content in Fe-Al melt by the addition of Fe<sub>2</sub>O<sub>3</sub> as an oxygen source. For the melts containing Al higher than 20 mass pct, CaO flux was added onto Al deoxidized melts to promote the removal of suspended Al<sub>2</sub>O<sub>3</sub> particles in the liquid iron. Equilibrium oxygen content in pure liquid Al contained in an Al<sub>2</sub>O<sub>3</sub> crucible was also determined at 1673 K, 1773 K, and 1873 K (1400 °C, 1500 °C, and 1600 °C).

#### A. Deoxidation by Al Addition in Fe-O Melt

The Al deoxidation equilibria were determined by adding Al into liquid iron. When the desired Al content is low, a pre-melted Fe-1 mass pct Al alloy was repeatedly added up to 0.04 mass pct Al in Fe-O melt initially containing very low oxygen as mentioned earlier. For higher Al contents, appropriate amount of pure Al shot (99.9 pct purity) was added up to

20 mass pct with samplings. After each addition, a new Al-O equilibrium was attained within 2 hours.

#### B. Oxidation of Al by Fe<sub>2</sub>O<sub>3</sub> Addition in Fe-Al Melt

In order to resolve the “oxygen deficiency” problem discussed in the preceding section, the Al-O relation at high Al content was also determined in such a way that Al was oxidized and decreased from its high content by the addition of Fe<sub>2</sub>O<sub>3</sub> as an oxygen source. A pre-melted Fe-9.06 mass pct Al alloy was charged and melted in a pure Al<sub>2</sub>O<sub>3</sub> crucible at 1873 K (1600 °C) under Ar-10 pct H<sub>2</sub> gas for 2 hours. The initial oxygen content in the melt prior to Fe<sub>2</sub>O<sub>3</sub> addition was 1.8 mass ppm. The gas was switched to dehydrated and deoxidized Ar gas, and a pre-determined amount of 14 g of Fe<sub>2</sub>O<sub>3</sub> powder to oxidize 1 mass pct of Al was added onto the Fe-Al alloy melt.

After the addition of  $\text{Fe}_2\text{O}_3$  powder, a thin layer of presumably  $\text{Al}_2\text{O}_3$  was immediately formed on the melt surface. Three hours of equilibration time was needed for the Al oxidation equilibrium as well as the floatation of the  $\text{Al}_2\text{O}_3$  inclusions from the melt.  $\text{Fe}_2\text{O}_3$  additions and samplings were repeated as long as the free metal surface was available for oxide additions. In some experiments, the  $\text{Fe}_2\text{O}_3$  addition was also made after the Al addition experiment.

### C. CaO Flux Addition to Remove $\text{Al}_2\text{O}_3$ Particles

In the present experiments, the reproducibility in the O analysis in the samples with high Al content ( $[\text{pct Al}] > 10$  mass pct) was poor. As will be shown in Section IV, it was attributed to the insoluble O from suspended  $\text{Al}_2\text{O}_3$  particles in liquid iron. Therefore, in order to remove these  $\text{Al}_2\text{O}_3$  particles effectively, a small amount of CaO flux was added onto the liquid iron after Al deoxidation to form a liquid CaO- $\text{Al}_2\text{O}_3$  oxide.

Thirty grams of pre-melted Fe-40 and 50 mass pct Al alloys or pure Al were charged in an  $\text{Al}_2\text{O}_3$  crucible (outer diameter [OD] 40 mm, inner diameter [ID] 30 mm, height [H] 50 mm) and melted under an Ar-10 pct  $\text{H}_2$  atmosphere using a 15 kW/50 kHz high-frequency induction furnace. After 2 hours of melting at desired temperatures, the gas was switched to dehydrated and deoxidized Ar gas, and 2 g of CaO flux was added onto the melt. After the addition of CaO flux, a liquid slag was immediately formed on the melt surface.

After 2 hours of equilibration, the top slag gradually solidified. The sample was then immediately quenched by helium gas stream and carefully sectioned for the chemical analysis.

### D. Sample Analyses

After every equilibration time of Al or  $\text{Fe}_2\text{O}_3$  addition experiments, a metal sample of about 20 g was extracted near the bottom of the melt by a 4-mm ID quartz tube connected to a syringe (10 mL), and it was quenched rapidly in ice water within 2 seconds. The metal samples were carefully cut for the chemical analysis. Generally, three to six specimens of each metal sample were prepared for the analysis of oxygen. The middle part of the cylindrical sample was used for the analysis of O. In case of CaO flux addition experiments, 30 g of the melt in an  $\text{Al}_2\text{O}_3$  crucible was quenched rapidly by helium gas blowing in the chamber. The center part of the sample was cross-sectioned to a plate shape and used for the O analysis.

The surface of the prepared samples was polished. After ultrasonic cleaning by the reagent grade of acetone, the oxygen content in the metal sample was measured by the inert gas fusion-infrared absorptiometry technique (LECO, TC-600), using the standard samples of steel containing 3, 10, and 26 mass ppm O. In order to check the gettering effect for high Al-containing samples, a Ni capsule was also used in the oxygen analysis.<sup>[1,25]</sup>

For the analysis of soluble Al content in metal sample, a piece of metal sample (0.2 g) was dissolved in 20 mL HCL(1 + 1) in a glass beaker of 50 mL

capacity heated in a water bath for 2 hours and analyzed by inductively coupled plasma-atomic emission spectrometry (ICP-AES, Spectro Analytical Instruments, SPECTRO ARCOS).

The inclusions formed in the liquid iron were also analyzed using the potentiostatic electrolytic extraction method. For the preparation of the 10 pct AA solution, 2.5 g of tetra-methyl ammonium was dissolved in 25 mL of acetyl acetone, and then 225 mL of methanol was added in a glass beaker with a capacity of 300 mL. One gram of the metal sample was dissolved in the 10 pct AA solution under a total electric charge of 300 mA for 6 hours. The inclusions were collected by the suction filtration using a membrane filter with an open pore size of 0.1  $\mu\text{m}$ . Morphology and composition of the inclusions were analyzed using scanning electron microscopy-energy dispersive X-ray spectroscopy (SEM-EDS, Hitachi, S4800).

The oxide layer formed on the melt surface with CaO flux additions was analyzed by the ICP-AES and also examined by the X-ray diffraction analysis (XRD, Rigaku, D/MAX-25000/PC) to identify the phases formed in liquid CaO- $\text{Al}_2\text{O}_3$  oxide during the dissolution of  $\text{Al}_2\text{O}_3$  particles.

## IV. EXPERIMENTAL RESULTS

Experimental Al and O contents measured in the present study are summarized in Tables II and III. In this section, the data from present research along with those available in the literature are presented and discussed, in particular for the reliability of the experimental techniques employed in the present study. Limitation of application of the WIPF is addressed with those experimental data in Section V. More detailed thermodynamic analysis will be presented in Part II of the present series.<sup>[23]</sup>

Figure 2 shows a representative deoxidation equilibria obtained in the present study at 1873 K (1600 °C). The dashed line is a best-fit line only for representation purpose and does not imply theoretically analyzed results.

In the region of the  $[\text{pct Al}]$  up to 17.3 mass pct, Fe-1 mass pct Al alloy or pure Al was added in liquid iron. The O content decreased with the increase of Al content and reached the minimum threshold value of about 2 mass ppm at  $[\text{pct Al}]$  of 0.71. Further addition of Al increases the O content which is in agreement with the previous reports.<sup>[3,7,8,11]</sup> During the Al deoxidation experiment, suspended  $\text{Al}_2\text{O}_3$  particles could be a source of overestimation of the O content in the measurement of Al-O relation in liquid iron. Also, the initial O content in electrolytic iron may affect the O content results of Al deoxidation experiment. In order to minimize this problem, the initial O content in the melt was controlled to ~10 mass ppm by Ar- $\text{H}_2$  gas blowing prior to Al addition. Strong agitation in the melt by the induction furnace also helped the fast attainment of deoxidation equilibrium as well as the floatation of the  $\text{Al}_2\text{O}_3$  inclusions from the melt.

**Table III. The Oxygen Solubility in Pure Liquid Al at 1673 K to 1873 K (1400 °C to 1600 °C)**

Temp. [K (°C)]	[pct O] in Pure Liquid Al							
	No CaO Addition				CaO Addition			
1873 (1600)	0.0134	0.0157	0.0195	0.0224	0.0247	0.0122	0.0129	0.0147
1773 (1500)	0.00898	0.0109	0.0149	0.0176	0.0188	0.00691	0.00817	0.00933
1673 (1400)	0.00530	0.0111	0.0119	0.0141	0.0169	0.00508	0.00774	0.00600

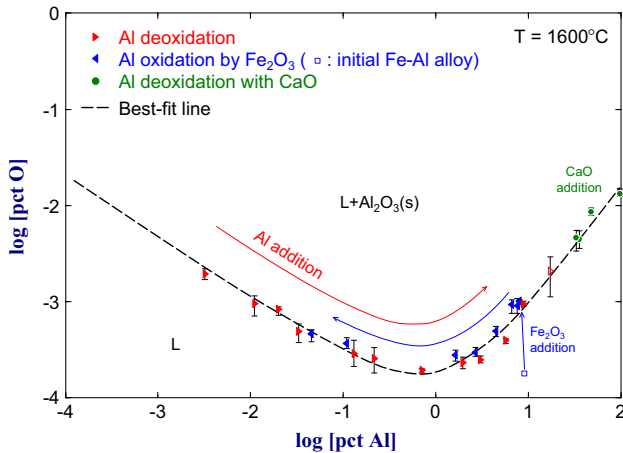


Fig. 2—Selected experimental data for the Al deoxidation equilibria at 1873 K (1600 °C) by different experimental methods.

In order to confirm the Al-O relations obtained from the Al addition experiment, and to resolve issues regarding “oxygen deficiency” problem at high Al content,<sup>[26]</sup> Fe<sub>2</sub>O<sub>3</sub> was added to a high Al-containing melt. The initial composition of the melt was Fe-9.06 mass pct Al-0.00018 mass pct O as marked by an open square in Figure 2. When a pre-determined amount of Fe<sub>2</sub>O<sub>3</sub> was added, [pct Al] decreased to 8.04, while [pct O] increased to 0.00098. Further additions of Fe<sub>2</sub>O<sub>3</sub> decreased the Al and O contents simultaneously along the best-fit line as shown in the figure. In some experiments, the Fe<sub>2</sub>O<sub>3</sub> addition was also made after the Al addition experiment. The experimental data of B-7 and B-8 in Table II are the results of Fe<sub>2</sub>O<sub>3</sub> additions to Fe-0.71 mass pct Al alloy after the Al addition experiment of A-7. The Al-O relations obtained by the Al oxidation in Fe-Al melt by Fe<sub>2</sub>O<sub>3</sub> are in excellent agreement with the relations obtained by the Al additions in liquid iron over a wide range of composition. This proves that the equilibria obtained in the present study are reproducible and reliable. This also lends a strong support that there was no oxygen deficiency problem in the melt at high Al concentration in the present study.

In the present study, the oxygen solubility was also measured for the Fe-Al melts containing initially 40 and 50 mass pct Al as well as pure liquid Al. A thin oxide layer, probably Al<sub>2</sub>O<sub>3</sub>, was formed on the surface of the melt during melting, and the layer did not completely disappear by Ar-H<sub>2</sub> gas blowing for a long period of time up to 4 hours. The oxygen analysis of the samples from these melts was not reproducible. For an example, the oxygen contents in pure liquid Al in equilibrium with

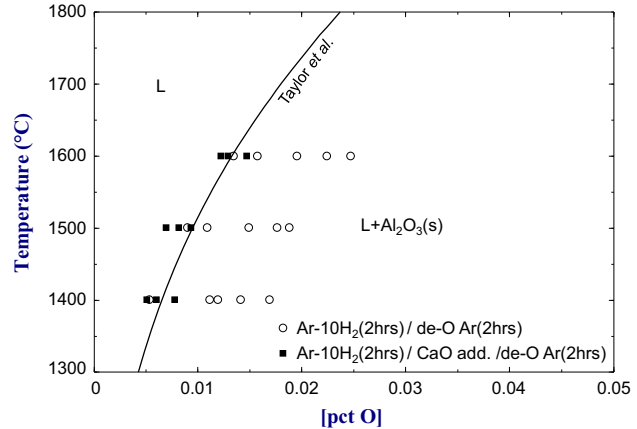


Fig. 3—The oxygen solubility in pure liquid Al at 1673 K to 1873 K (1400 °C to 1600 °C): Solid line is a solubility limit calculated by Taylor *et al.*<sup>[30]</sup>

Al<sub>2</sub>O<sub>3</sub> determined in the present study in the temperature range from 1673 K to 1873 K (1400 °C to 1600 °C) are plotted in Figure 3 as open circles. The oxygen content was highly scattered, and the uncertainty was more than 0.01 mass pct at 1873 K (1600 °C). This may be attributed to suspended Al<sub>2</sub>O<sub>3</sub> particles in the Al melt as shown in Figures 4(a) and (c). The poor reproducibility in the O analysis in Fe-Al alloy samples with Al contents of 40 and 50 mass pct can be also attributed to the same reason.

In order to resolve this problem, it was essential to minimize the Al<sub>2</sub>O<sub>3</sub> particles suspended in the melt during the Al-O equilibration experiments. In the present study, CaO flux was added onto the melt as described in Section III-C. As a result, a liquid CaO-Al<sub>2</sub>O<sub>3</sub> layer was formed and played a role of absorbing Al<sub>2</sub>O<sub>3</sub> particles suspended in the melts. As can be seen in Figures 4(b) and (d), only few numbers of small-sized Al<sub>2</sub>O<sub>3</sub> inclusions (~0.2 μm) were observed in a quenched Al melt. The oxygen contents of these samples were much less scattered as marked by solid squares in Figure 3, and they were considered to be more accurate than those obtained from the samples without CaO flux addition. The oxygen contents in pure Al melt determined in the present study in the temperature range from 1673 K to 1873 K (1400 °C to 1600 °C) are in good agreement with the O solubility limit in pure Al melt calculated by Taylor *et al.*<sup>[30]</sup> as shown in the figure. The Al-O relations in Fe-36.6 and 49.0 mass pct Al alloy melts are also shown in Figure 2, and they show a good correlation with other data with the discrepancy of the oxygen analysis of ±5 mass ppm.

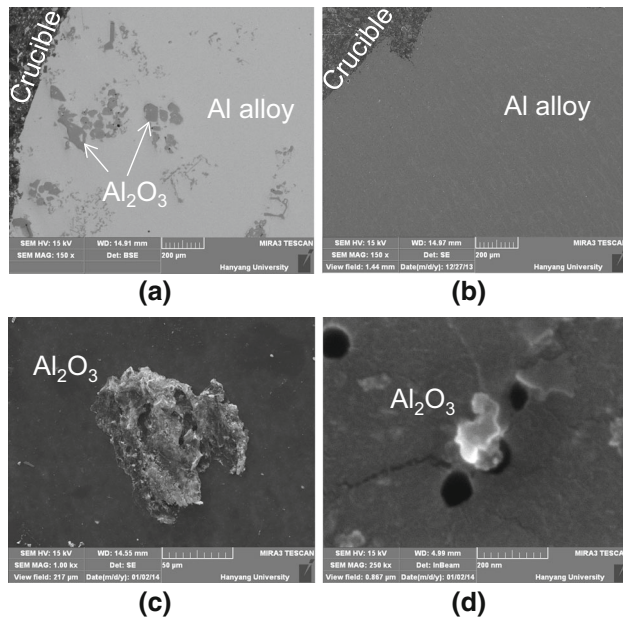


Fig. 4—SEM images of quenched Al melt samples and suspended alumina particles: (a), (c) without CaO pellet addition; (b), (d) with CaO pellet addition.

Figure 5 shows the phase diagram of CaO-Al<sub>2</sub>O<sub>3</sub> system along with the final composition of the formed slag for the CaO flux addition experiments. The Al<sub>2</sub>O<sub>3</sub> contents in CaO-Al<sub>2</sub>O<sub>3</sub> slag were 62.83 mass pct Al<sub>2</sub>O<sub>3</sub> at 1873 K (1600 °C) for Fe-36.6 mass pct Al alloy and 51.67 mass pct at 1673 K (1400 °C) for pure Al, respectively. The slags were saturated with calcium aluminate (CaO·Al<sub>2</sub>O<sub>3</sub>) phase, and also contained pure Al<sub>2</sub>O<sub>3</sub> as shown by the XRD analysis in Figure 6. The main oxide phases formed on the surface of Fe-36.6 mass pct Al alloy melt are CaO·Al<sub>2</sub>O<sub>3</sub> and pure Al<sub>2</sub>O<sub>3</sub> indicating that the oxide layer on the melt surface is composed of a low melting CaO-Al<sub>2</sub>O<sub>3</sub> phase and Al<sub>2</sub>O<sub>3</sub> particles. Also as shown in Figure 7, the oxide inclusions extracted from Fe-36.6 mass pct Al melt were identified as pure Al<sub>2</sub>O<sub>3</sub> by the SEM-EDS analysis. Therefore, it can be concluded that the alloy melts containing high Al and pure Al melt with a CaO flux addition are in equilibrium with pure solid Al<sub>2</sub>O<sub>3</sub> ( $a_{\text{Al}_2\text{O}_3} = 1$ ) under the present experimental condition.

The Al-O relation in liquid iron at 1923 K (1650 °C) was also measured by the addition of Al in Fe-O melts, and the results are summarized in Table II. The data will be used to discuss the temperature dependence of Al deoxidation equilibria in liquid iron in the subsequent article of this series.<sup>[23]</sup>

## V. DISCUSSION

### A. The Al-O Relation in Liquid Iron at 1873 K (1600 °C)

The Al-O relation in liquid iron measured in the present study as well as those available in literature is compared in Figure 8. While there are considerable

scatters in the literature data, the present experimental results are in good agreement with the lower [pct O] values of the previous data over the whole Al composition range at 1873 K (1600 °C).

Figure 9 shows the same relation at high Al concentration region ( $0.1 < [\text{pct Al}] < 100$ ) including the previous model predictions.<sup>[5,10,11,13,16]</sup> The result obtained in the present study is partly in agreement with that of Kang *et al.*<sup>[11]</sup> Suito *et al.*,<sup>[8]</sup> and Shevtsov.<sup>[7]</sup> While Kang *et al.*<sup>[11]</sup> did not use any flux to absorb Al<sub>2</sub>O<sub>3</sub> particles, Suito *et al.*<sup>[8]</sup> employed CaO-Al<sub>2</sub>O<sub>3</sub> flux to absorb the Al<sub>2</sub>O<sub>3</sub> particles. From the agreement between these reports<sup>[8,11]</sup> as well as the result in the present study, it is thought that the addition of CaO flux did not deteriorate the Al deoxidation equilibria in Fe-Al-O melts saturated with pure Al<sub>2</sub>O<sub>3</sub> ( $a_{\text{Al}_2\text{O}_3} = 1$ ). For the Al-rich side in the Fe-Al alloy system, the only available data for the Al-O relation can be found in Shevtsov's work.<sup>[7]</sup> In the preliminary experiments in the present study, the metal samples obtained from the Al-rich melts containing Al over 50 mass pct were too brittle to prepare the samples for the O analysis. The present results of the oxygen contents in Fe-33.2 mass pct Al, Fe-36.6 mass pct Al, and Fe-49.0 mass pct Al samples are in good agreement with Shevtsov's data.<sup>[7]</sup>

### B. Thermodynamic Description by the Interaction Parameter Formalism

The lines shown in Figures 1 and 9 are the model calculations reported in previous studies, mostly using WIPF, except for that of Jung *et al.* using UIPF with associate.<sup>[16]</sup> As shown in Figure 1, most of model calculations showed a reasonable agreement when [pct Al] is lower than 0.1 mass pct. However, very different predictions can be seen at higher Al concentration. A recent application of the WIPF by Kang *et al.*<sup>[11]</sup> to the deoxidation equilibria at high Al content shows a good agreement with their own measurement up to ~10 mass pct of Al, but their model could not account for the most of previous experimental data at low Al content.

As shown in the figures, there has been no accurate prediction of the Al deoxidation equilibria applicable to whole concentration range from very low Al content to almost pure liquid Al. This is mainly because (1) the WIPF is, in principle, only applicable to infinite dilute solutions,<sup>[28]</sup> (2) ignoring very strong interaction between Al and O. In the following discussion, it will be shown that these two problems cannot be properly accounted for by the WIPF, in particular for the situation when one wants to model the deoxidation equilibria in entire concentration region.

In a standard procedure to interpret the deoxidation equilibria, the equilibrium constant of Reaction [1], and the first-order interaction parameter,  $e_{\text{O}}^{\text{Al}}$ , are determined simultaneously. Using the Lupis' reciprocal relationship,<sup>[20]</sup> Eq. [3] can be rearranged as

$$\begin{aligned}
 & -2e_{\text{Al}}^{\text{Al}}[\text{pctAl}] - 3e_{\text{O}}^{\text{O}}[\text{pctO}] - \log[\text{pctAl}]^2[\text{pctO}]^3 \\
 & = -\log K + (3[\text{pctAl}] + 3.38[\text{pctO}])e_{\text{O}}^{\text{Al}}
 \end{aligned} \quad [7]$$



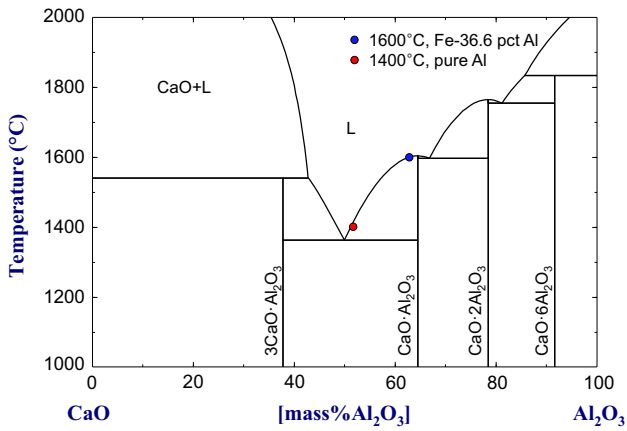


Fig. 5—CaO-Al<sub>2</sub>O<sub>3</sub> binary phase diagram along with final composition of slag.

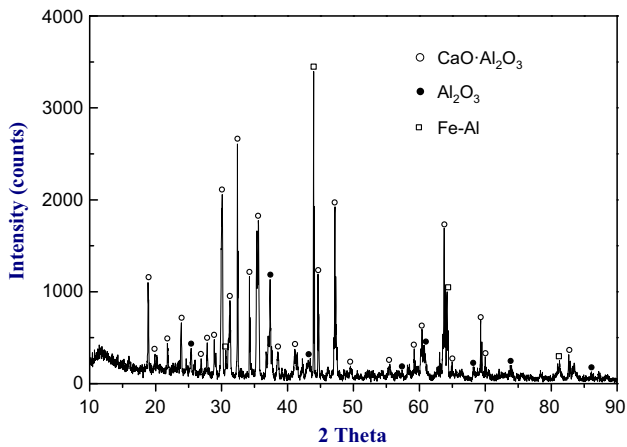
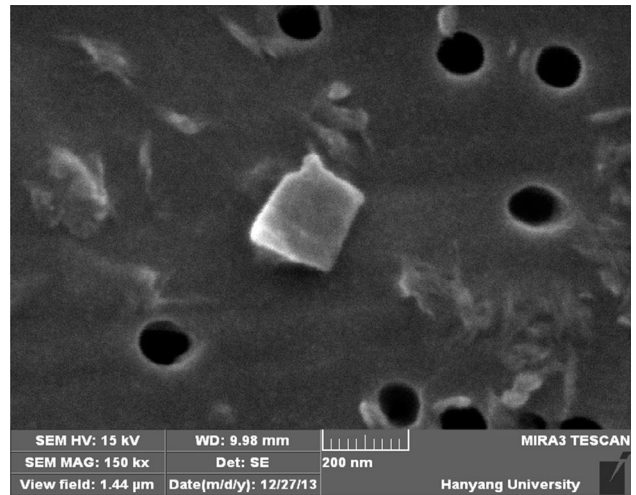
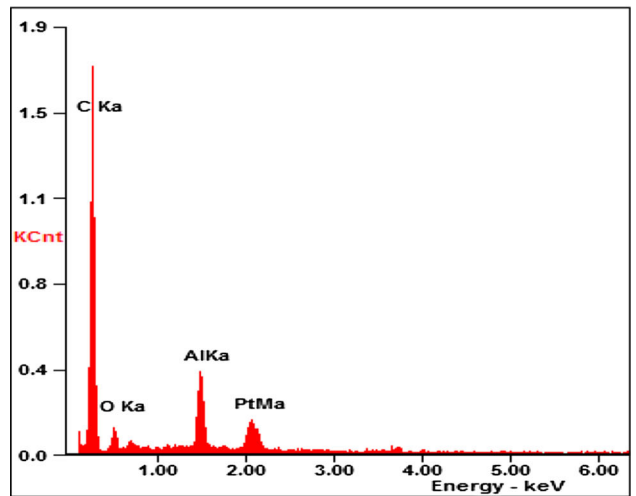


Fig. 6—XRD data of oxides formed on the surface of Fe-36.6 mass pct Al alloy melt.

where the self-interaction parameters of Al and O in liquid iron,  $e_{Al}^{Al} (= 80.5/T)$  and  $e_O^O (= -1750/T + 0.76)$ , were taken from JSPS.<sup>[27]</sup> The left-hand side of Eq. [7] is plotted vs  $(3[\text{pct Al}] + 3.38[\text{pct O}])$ , and the  $K$  and the  $e_O^{Al}$  are simultaneously obtained by taking an intercept at  $y$ -axis and slope of the plot, provided that the experimental deoxidation data could be well represented by Eq. [7]. One such plot is shown in Figure 10 using all available experimental data including those of the present study. As can be seen, the plot does not show a linear function of  $(3[\text{pct Al}] + 3.38[\text{pct O}])$  over a wide concentration range. Only very limited composition range would be represented by a linear plot, even at the low [pct Al] up to 1 mass pct as shown in Figure 10(a). Each author has reported their own choices of combination ( $K$  and  $e_O^{Al}$ ) in order to best represent some selected data. When this analysis is done in more wide concentration range up to 100 pct Al content (Figure 10(b)), it is clearly seen that the experimental data cannot be explained by any linear plot of different combination of  $K$  and  $e_O^{Al}$ . For a description of this



(a)



(b)

Fig. 7—(a) SEM image and (b) EDS spectrum of inclusion in Fe-36.6 mass pct Al alloy.

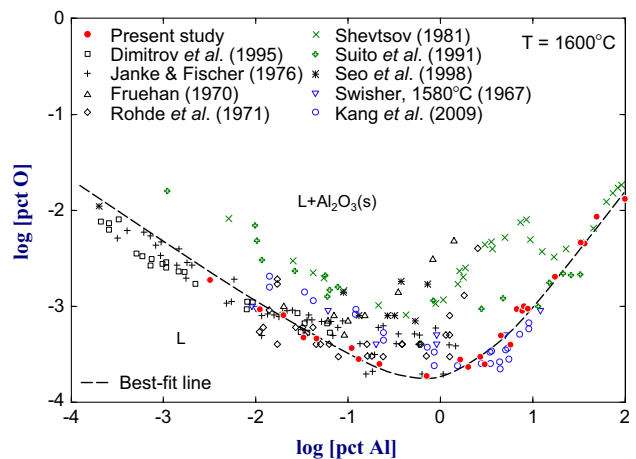


Fig. 8—The Al-O relations in Fe-Al melts at 1873 K (1600 °C) from very low Al to pure liquid Al: A dashed line is only to guide eye.

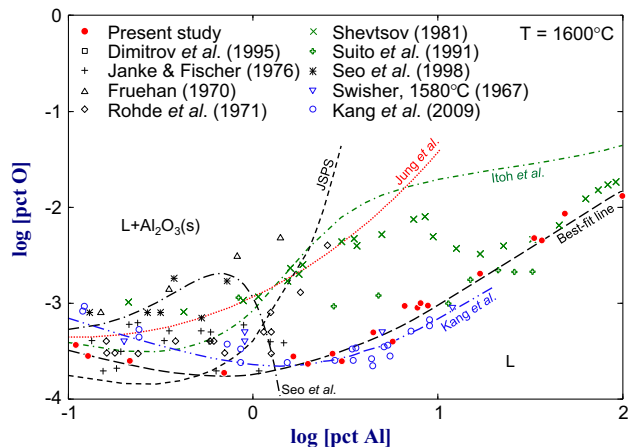


Fig. 9—The Al-O relations in Fe-Al melts at 1873 K (1600 °C) at Al concentration range from 0.1 to 100 mass pct together with previous model predictions.<sup>[5,10,11,13,16]</sup>

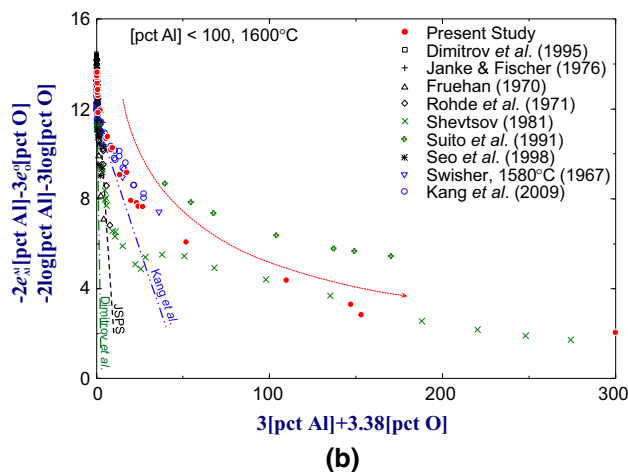
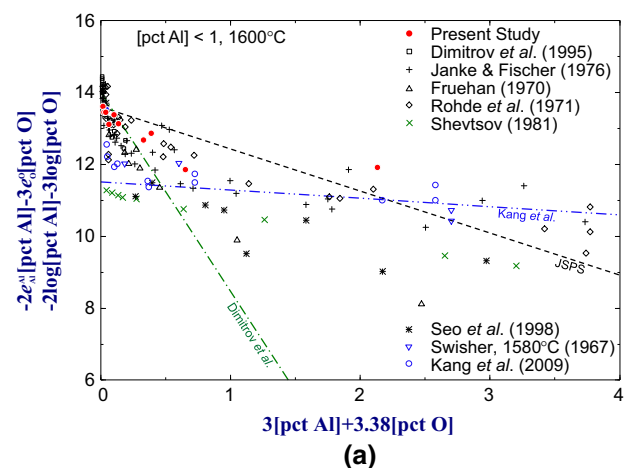


Fig. 10—Relation of Eq. [7] plotted against (3[pct Al] + 3.38[pct O]) (a) up to 1 mass pct Al and (b) up to 100 mass pct Al.

nonlinear behavior, Gustafsson and Mellberg<sup>[14]</sup> proposed to use the second-order polynomial of (3[pct Al] + 3.38[pct O])<sup>2</sup>. However, it was the temporary

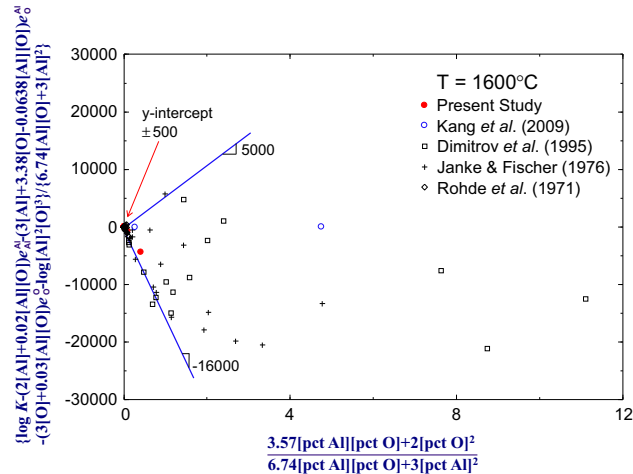


Fig. 11—Relation of Eq. [4] plotted against  $\frac{3.57[\text{pct Al}][\text{pct O}] + 2[\text{pct O}]^2}{6.74[\text{pct Al}][\text{pct O}] + 3[\text{pct Al}]^2}$ .

expedient for the low Al concentration region, and there is no physical background.

In order to extend the applicability of the formalism at high Al concentration region, several researchers<sup>[10,11,13]</sup> used the second-order interaction parameters. Using Eq. [4], the  $r_{\text{Al}}^{\text{Al}}$  and  $r_{\text{Al}}^{\text{O}}$  values can be determined from the intercept of y-axis and slope, respectively. However, too much scatter in the plot prevents determination of meaningful parameters, as shown in Figure 11. The  $r_{\text{Al}}^{\text{Al}}$  represented by the intercept of the y-axis varies in the range of  $-500$  to  $+500$ , while  $r_{\text{Al}}^{\text{O}}$  represented by the slope varies from  $-16,000$  to  $5000$ .

To overcome the poor description of the WIPF, the two limitations mentioned previously should be resolved. The strong interaction between Al and O was reasonably treated by Bouchard and Bale,<sup>[15]</sup> and Jung *et al.*<sup>[16]</sup> by introducing associates and they could get significantly improved representation of the Al deoxidation equilibria. However, they considered the associates in the framework of the UIPF, which is thermodynamically consistent for whole concentration range only when some special relations are satisfied between Henrian activity coefficient of solute Al ( $\gamma_{\text{Al}}^{\circ}$ ) and interaction parameter  $\epsilon_{\text{AlAl}}$  ( $\epsilon_{\text{AlAl}} = -2 \ln \gamma_{\text{Al}}^{\circ}$ ).<sup>[28,31]</sup> In the next article of the present series (Part II),<sup>[23]</sup> it will be shown how this could be simultaneously solved. A thermodynamic model which can be applicable to entire concentration range will be employed. Moreover, the random mixing between components is no more assumed, but the strong interaction will be treated by a quasichemical approximation for the configurational entropy of mixing.<sup>[32]</sup> A detailed procedure of thermodynamic modeling of the liquid solution in the Fe-Al-O system will be reported.<sup>[23]</sup>

## VI. CONCLUSIONS

The Al deoxidation equilibria in liquid iron were investigated over the whole composition range

(0.0027 < [pct Al] < 100) at 1873 K and 1923 K (1600 °C and 1650 °C). Literature survey revealed that (1) the accurate Al deoxidation equilibria in liquid iron at high Al concentration are required, and (2) a better thermodynamic model is necessary to account for the deoxidation equilibria. A series of experiments were carried out to determine the Al deoxidation equilibria in liquid iron. In particular, in order to obtain accurate equilibrium results, three different experimental techniques were employed namely, (1) deoxidation by the additions of Al, (2) Al oxidation by the addition of Fe<sub>2</sub>O<sub>3</sub>, and (3) the addition of CaO flux, depending on the Al content in liquid iron. Obtained experimental data were in agreement with the previously reported data in literature in such a way that the present experimental results agree with the reported data of lower O content. The equilibrium data were compared with available model calculations using WIPF and UIPF with associates. It was pointed out that the previous modeling approach could not account for the deoxidation equilibria at high Al content. A new thermodynamic modeling to account for the Al deoxidation equilibria will be reported in a subsequent article.<sup>[23]</sup>

#### ACKNOWLEDGMENT

This study was supported by the R&D Center for Valuable Recycling (Global-Top Environmental Technology Development Program) funded by the Ministry of Environment (Project No.: 11-C22-ID).

#### REFERENCES

1. N.A. Gokcen and J. Chipman: *J. Met.*, 1953, vol. 197, pp. 173–78.
2. A. McLean and H.B. Bell: *J. Iron Steel Inst.*, 1965, vol. 203, pp. 123–30.
3. J.H. Swisher: *Trans. Metall. Soc. AIME*, 1967, vol. 239, pp. 123–24.
4. R.J. Fruehan: *Metall. Trans.*, 1970, vol. 1, pp. 3403–10.
5. L.E. Rohde, A. Choudhury, and M. Wahlster: *Arch. Eisenhüttenwes.*, 1971, vol. 42, pp. 165–74.
6. D. Janke and W.A. Fischer: *Arch. Eisenhüttenwes.*, 1976, vol. 47, pp. 195–98.
7. V.E. Shevtsov: *Russ. Metall.*, 1981, vol. 1, pp. 52–57.
8. H. Suito, H. Inoue, and R. Inoue: *ISIJ Int.*, 1991, vol. 31, pp. 1381–88.
9. S. Dimitrov, A. Weyl, and D. Janke: *Steel Res.*, 1995, vol. 66, pp. 3–7.
10. J.D. Seo, S.H. Kim, and K.R. Lee: *Steel Res.*, 1998, vol. 69, pp. 49–53.
11. Y.J. Kang, M. Thunman, D. Sichen, T. Morohoshi, K. Mizukami, and K. Morita: *ISIJ Int.*, 2009, vol. 49, pp. 1483–89.
12. G.R. St Pierre: *Metall. Trans. B*, 1977, vol. 8B, pp. 215–17.
13. H. Itoh, M. Hino, and S. Banya: *Tetsu-to-Hagané*, 1997, vol. 83, pp. 773–78.
14. S. Gustafsson and P.O. Mellberg: *Scand. J. Metallurgy*, 1980, vol. 9, pp. 111–16.
15. D. Bouchard and C.W. Bale: *J. Phase Equilib.*, 1995, vol. 16, pp. 16–23.
16. I.H. Jung, S.A. Decterov, and A.D. Pelton: *Metall. Mater. Trans. B*, 2004, vol. 35B, pp. 493–507.
17. J.S. Kim, J.B. Jeon, J.E. Jung, K.K. Um, and Y.W. Chang: *Met. Mater. Int.*, 2014, vol. 20, pp. 41–47.
18. B.H. Song, J. Kim, S. Jeong, I. Choi, and Y.K. Lee: *Korean J Met. Mater.*, 2014, vol. 52, pp. 1–9.
19. J.H. Park, D.J. Kim, and D.J. Min: *Metall. Mater. Trans. A*, 2012, vol. 43A, pp. 2316–24.
20. C.H.P. Lupis and J.F. Elliott: *Acta Metall.*, 1966, vol. 14, pp. 529–38.
21. C. Wagner: *Thermodynamics of Alloys*, Addison-Wesley Press, Cambridge, MA, 1952, pp. 47–51.
22. J. Chipman: *The Physical Chemistry of Liquid Steel, in Basic Open-Hearth Steel Making*, The American Institute of Mining and Metallurgical Engineers, New York, 1951.
23. M.K. Paek, J.J. Pak, and Y.-B. Kang: *Metall. Mater. Trans. B*, 2015. DOI:10.1007/s11663-015-0369-z.
24. M.K. Paek, K.H. Do, Y.-B. Kang, I.H. Jung, and J.J. Pak: unpublished research.
25. R. Inoue and H. Suito: *Mater. Trans., JIM*, 1991, vol. 32, pp. 1164–69.
26. H. Yin: *Proc. of Int. Conf. of AISTech 2005*, vol. 2, Warrendale, PA, 2005, pp. 89–97.
27. The 19th Committee in Steelmaking: *Thermodynamic Data For Steelmaking*, The Japan Society for Promotion of Science, Tohoku University Press, Sendai, Japan, 2010, pp. 10–13.
28. L.S. Darken: *Trans. AIME*, 1967, vol. 239, pp. 80–89.
29. A.D. Pelton and C.W. Bale: *Metall. Trans. A*, 1986, vol. 17A, pp. 1211–15.
30. J.R. Taylor, A.T. Dinsdale, M. Hillert, and M. Selleby: *CAL-PHAD*, 1992, vol. 16, pp. 173–79.
31. A.D. Pelton: *Metall. Mater. Trans. B*, 1997, vol. 28B, pp. 869–76.
32. A.D. Pelton and P. Chartrand: *Metall. Mater. Trans. A*, 2001, vol. 32A, pp. 1355–60.